Powder X-ray diffraction data for all compounds were collected on a Philips powder diffractometer using CuK_α-radiation, graphite monochromator on diffracted beam and operating at 40 kV, 30 mA at 293 K.

Differential Scanning Calorimetry scans were done on a Mettler Toledo 422^e on **2** and a Thermal Analysis DSC-Q10 for **1** and **3.**
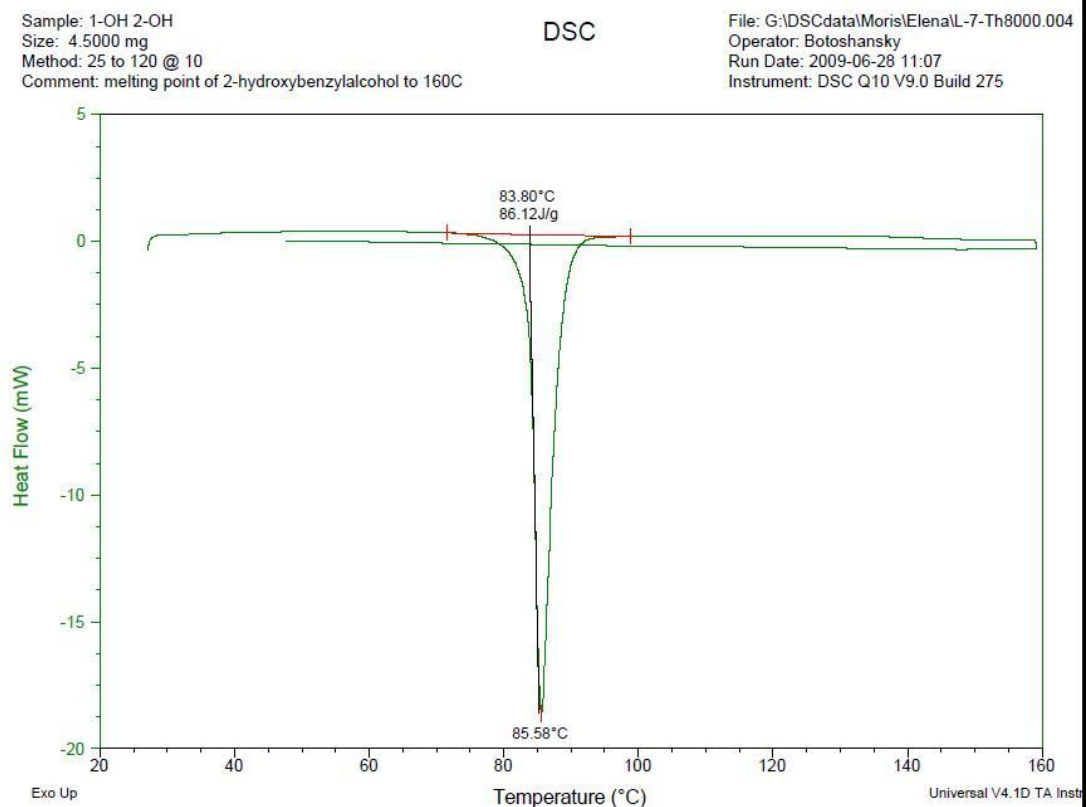
1) 2-methylolphenol (1)

Figure S1: DSC trace for 2-methylolphenol.
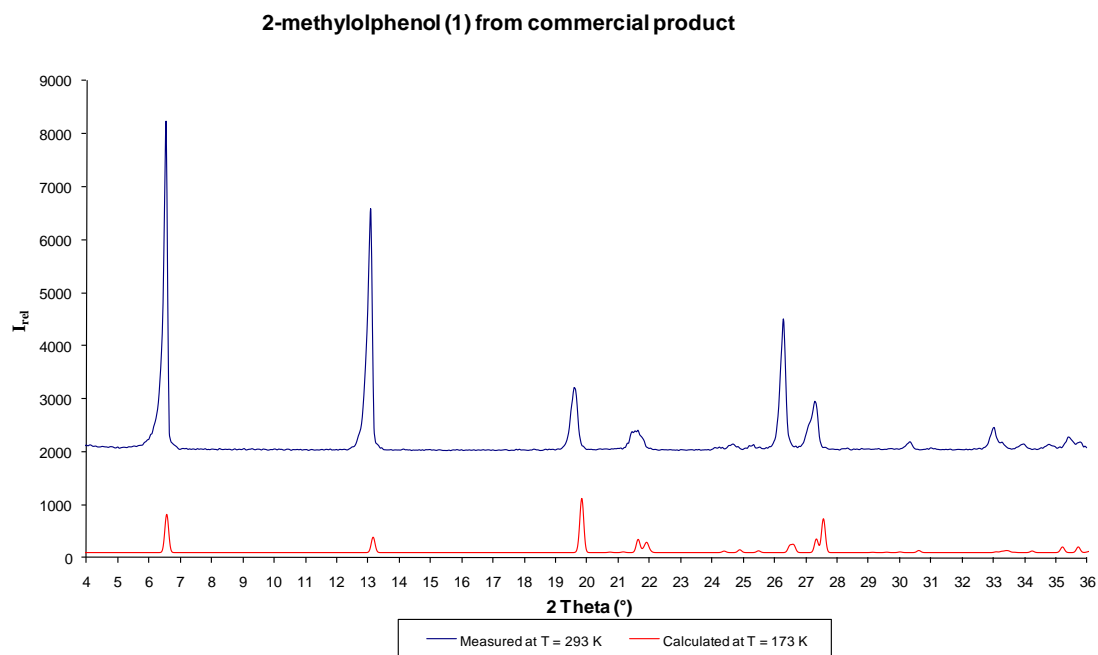
2-methylolphenol (1) from commercial product

Figure S2: Comparison of powder pattern obtained from commercial product and that calculated from the single crystal structure.
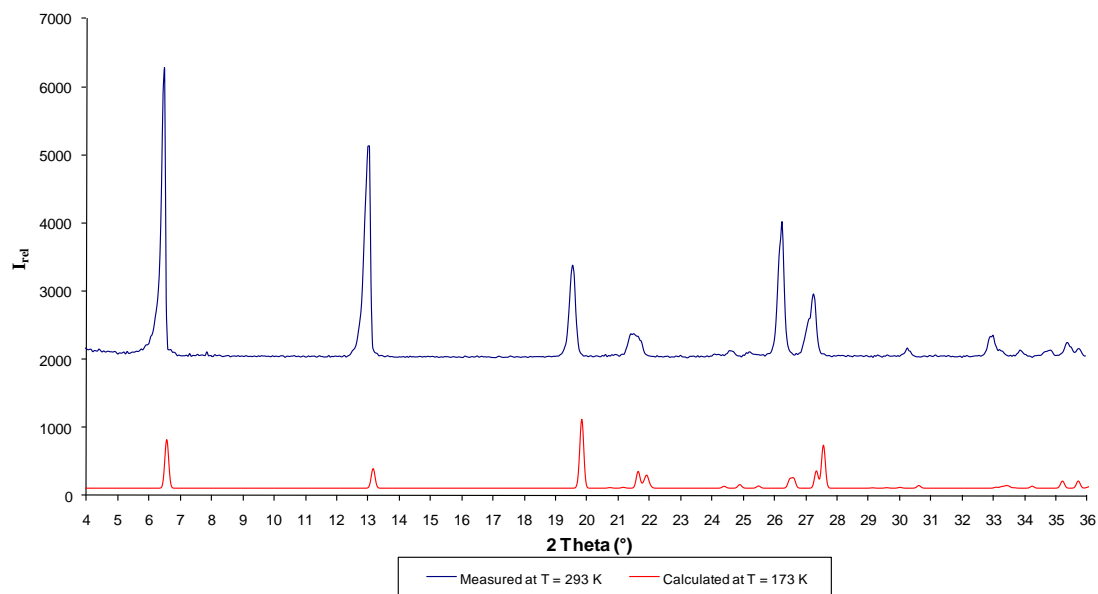
2-methylolphenol (1) from methanol

Figure S3: Comparison of powder pattern of crystals grown from methanol and that calculated from the single crystal structure for (**1**).

2-methylolphenol (1) from ethanol
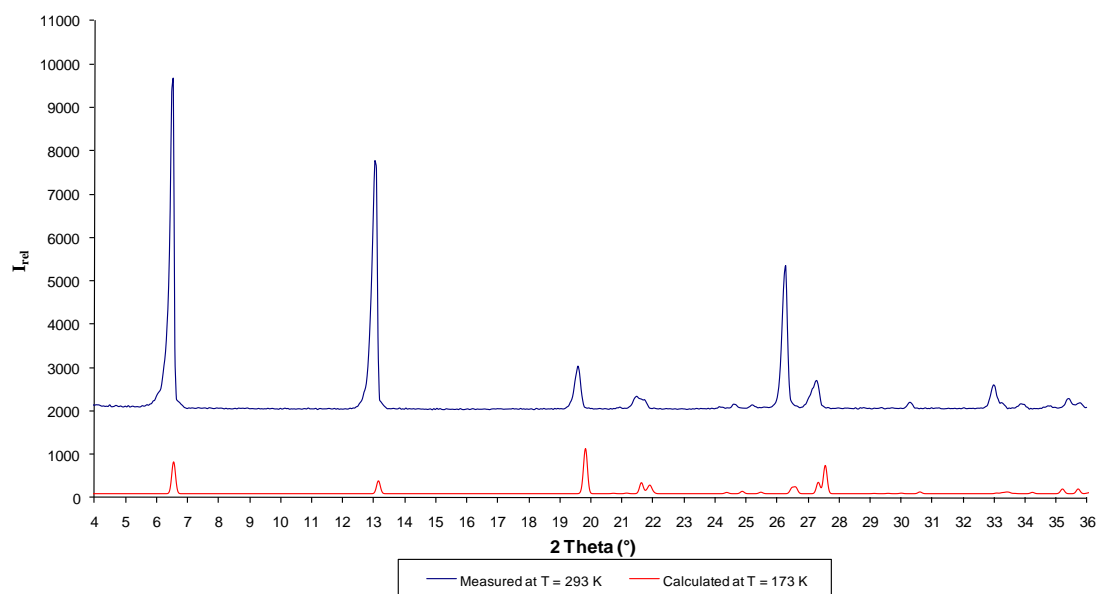

Figure S4: Comparison of powder pattern of crystals grown from ethanol and that calculated from the single crystal structure for (**1**).
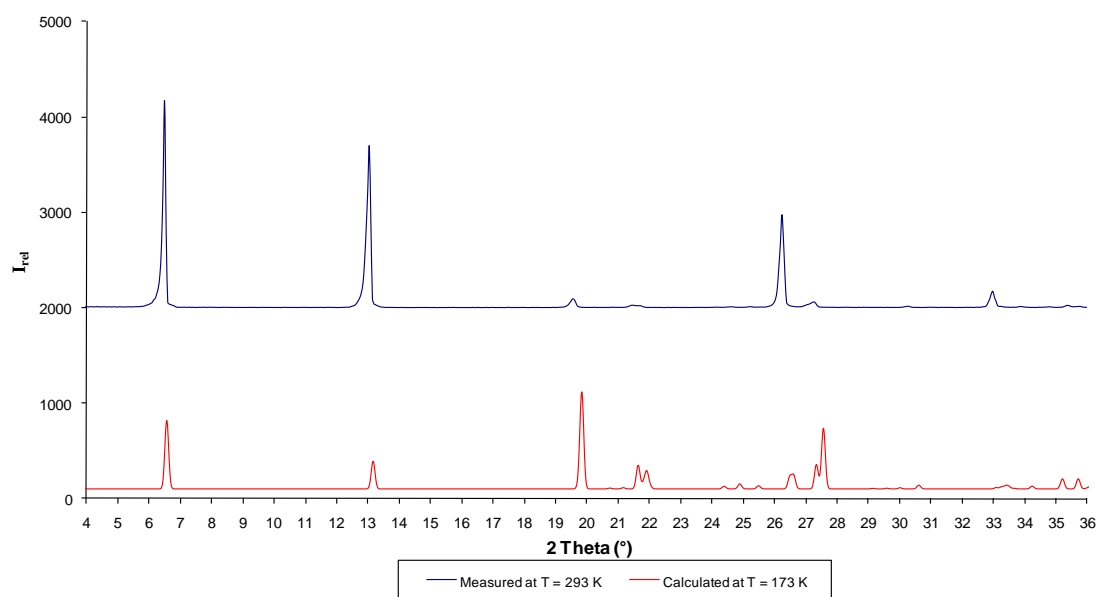
3

2-methylolphenol (1) from tetrahydrofuran

Figure S5: Comparison of powder pattern of crystals grown from tetrahydrofuran and that calculated from the single crystal structure for (**1**).
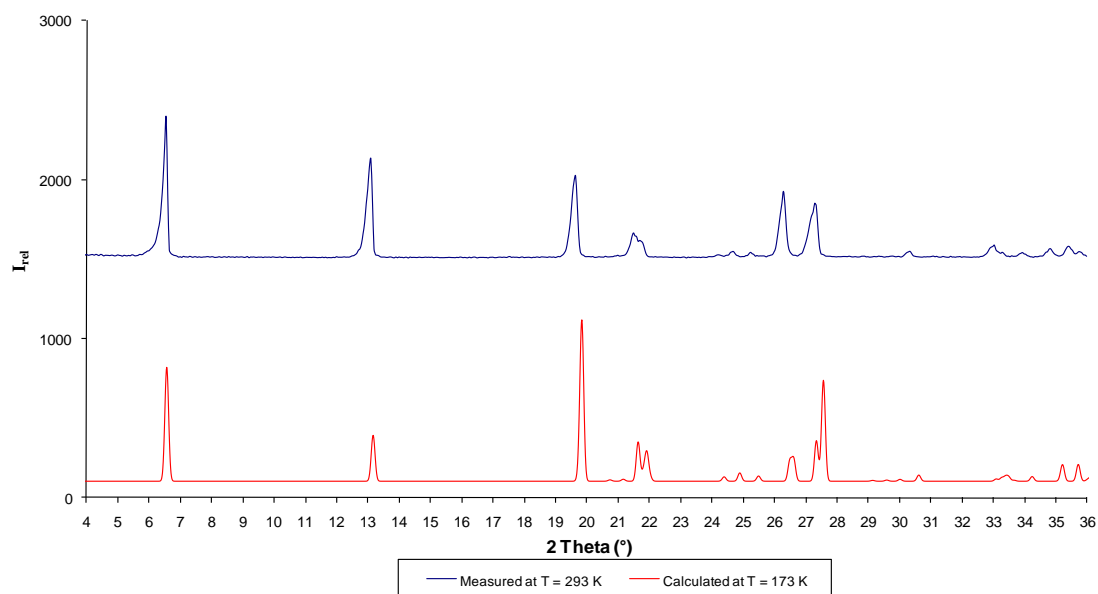
2-methylolphenol (1) from acetone

Figure S6: Comparison of powder pattern of crystals grown from acetone and that calculated from the single crystal structure for (**1**).
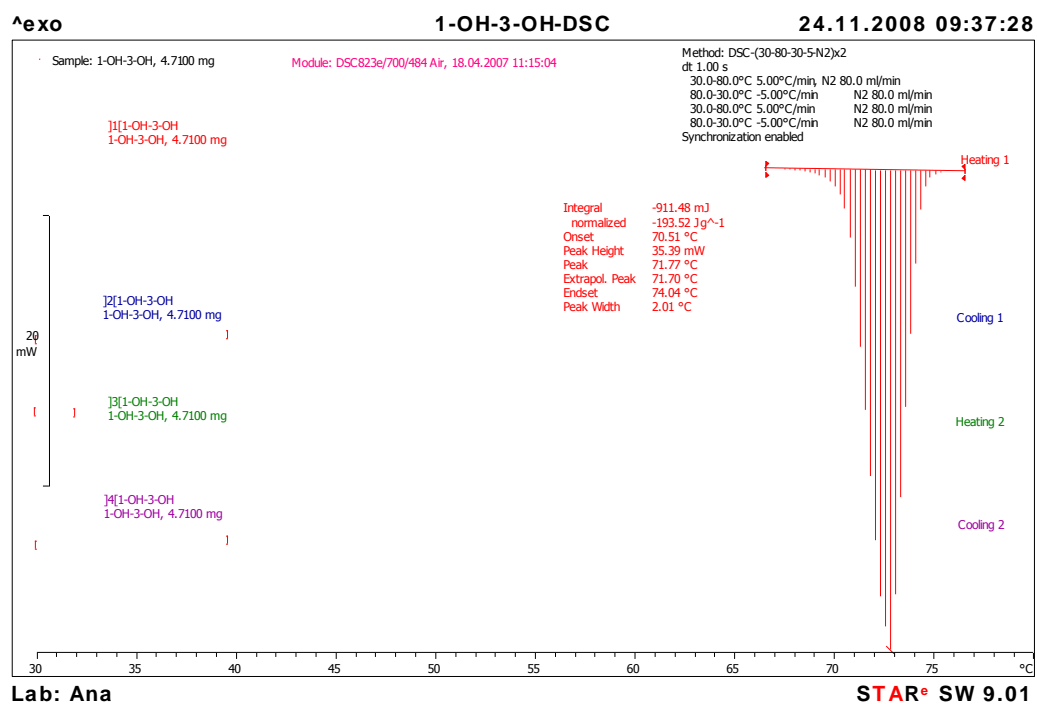
2) 3-methylolphenol (2)

Figure S7: DSC trace of commercial product.

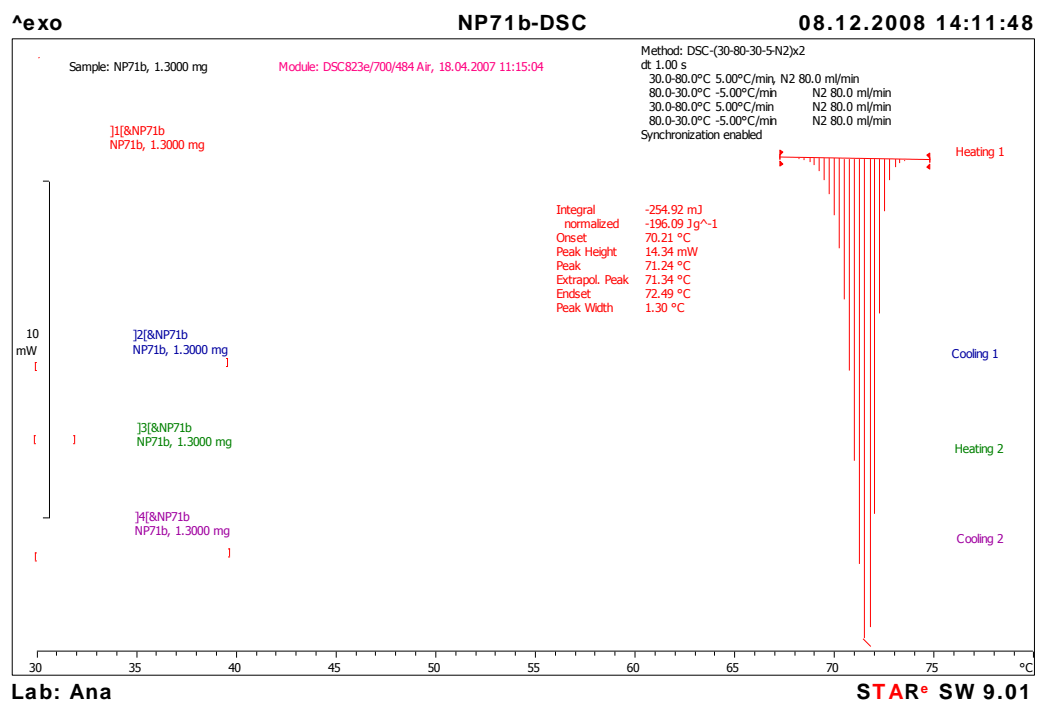Figure S8: DSC trace for Z' = 2 (**2a**).
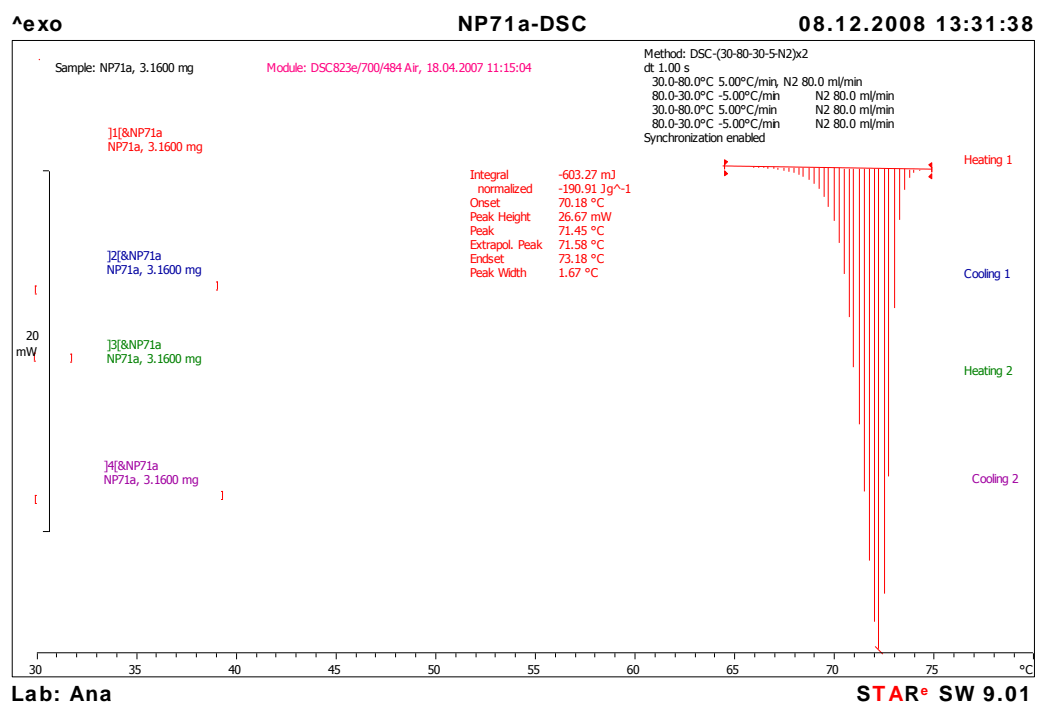
Figure S9: DSC trace for Z' = 3 (**2b**).

The major differences between the two polymorphs is in the peaks at $2\theta = 6.5°$, $18.5°$, $19.5°$, which are absent in the Z' = 2 polymorph, as shown below:

Figure S10: Comparison of powder pattern obtained from bulk material grown from methanol and that calculated from the single crystal structure for Z' = 2 (**2a**).
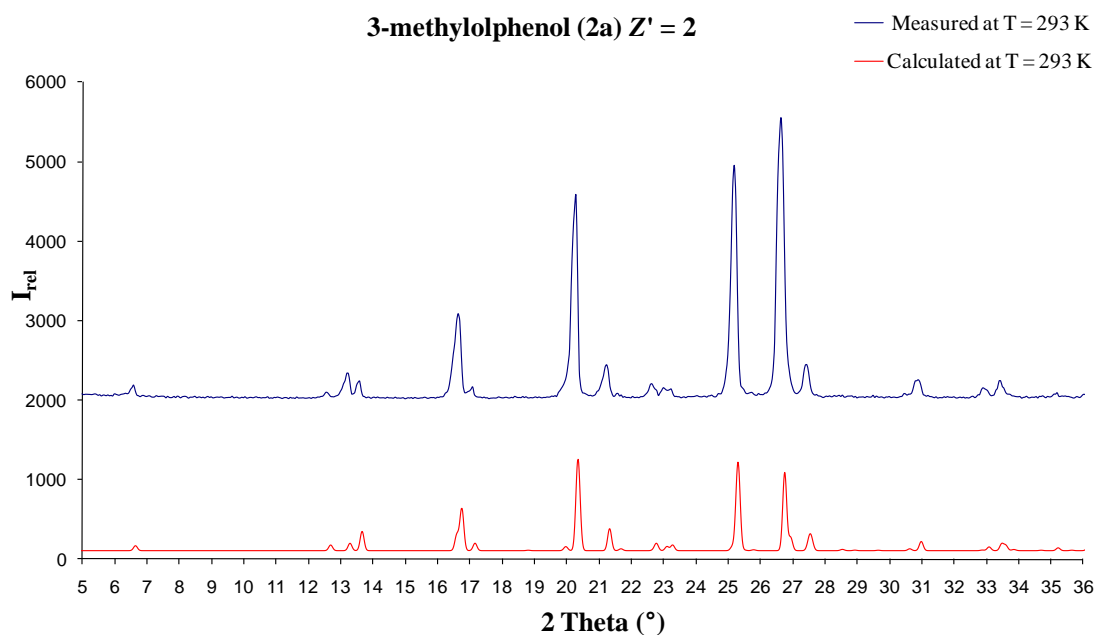
3-methylolphenol (2b) Z' = 3

Figure S11: Comparison of powder pattern obtained from bulk material grown from methanol and that calculated from the single crystal structure for Z' = 3 (**2b**).

3-methylolphenol (2b) *Z*' = 3

Figure S12: Comparison of powder pattern obtained from commercial product and that calculated from the single crystal structure of **2b**. Confirms that Z' = 3 is the commercially available polymorph.

The Z' = 3 polymorph was obtained from other slow evaporation crystallizations, using the solvents ethyl acetate, ethanol, acetone and tetrahydrofuran, shown below:

3-methylolphenol (2b) Z' = 3 from ethyl acetate
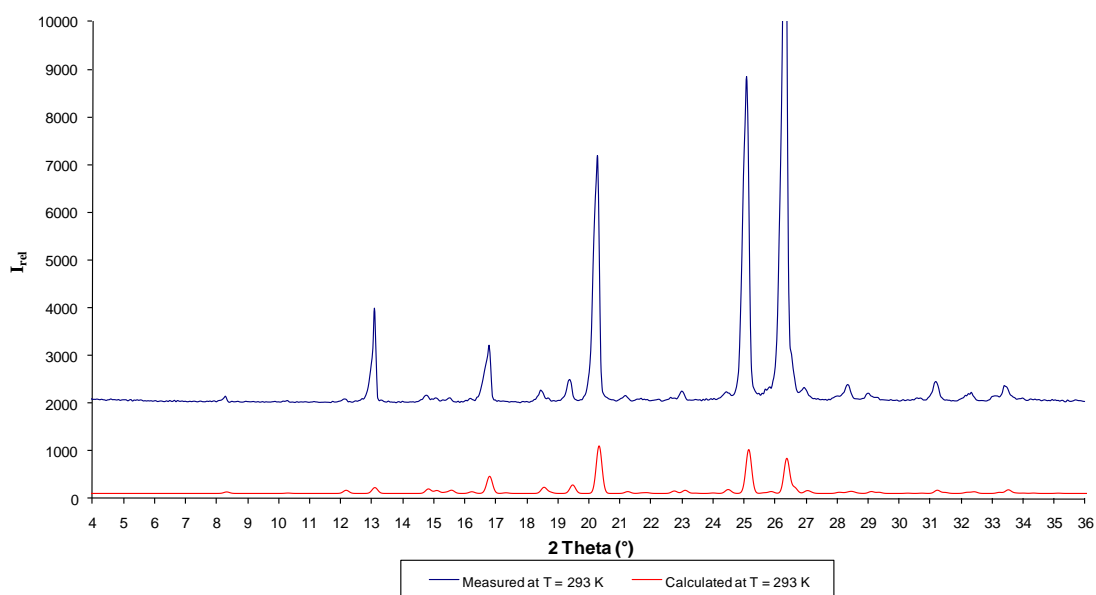
Figure S13: Comparison of powder pattern of crystals grown from ethyl acetate and that calculated from the single crystal structure for Z' = 3 (**2b**).
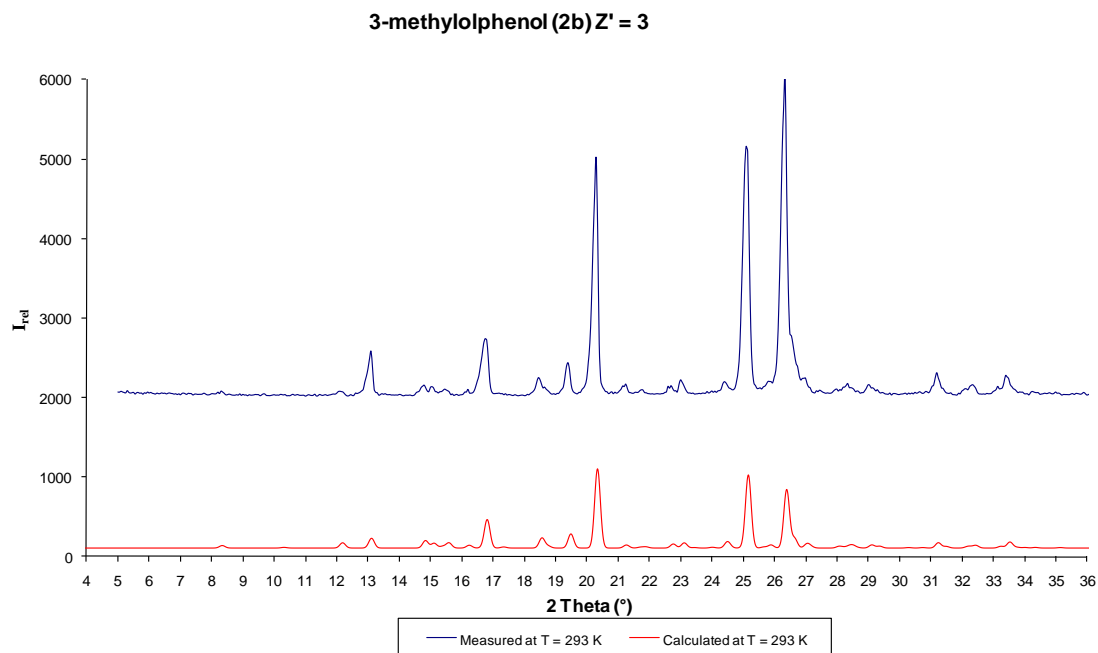
2-methylolphenol Z' = 3 from ethanol

Figure S14: Comparison of powder pattern of crystals grown from ethanol and that calculated from the single crystal structure for Z' = 3 (**2b**).

2-methylolphenol (2b) Z' = 3 from acetone

Figure S15: Comparison of powder pattern of crystals grown from acetone and that calculated from the single crystal structure for Z' = 3 (**2b**).

3-methylolphenol (2b) Z' = 3 from tetrahydrofuran

Figure S16: Comparison of powder pattern of crystals grown from tetrahydrofuran and that calculated from the single crystal structure for Z' = 3 (**2b**).

9

3) 4-methylolphenol (3)

Figure S17: DSC trace 4-hydroxybenzyl alcohol.
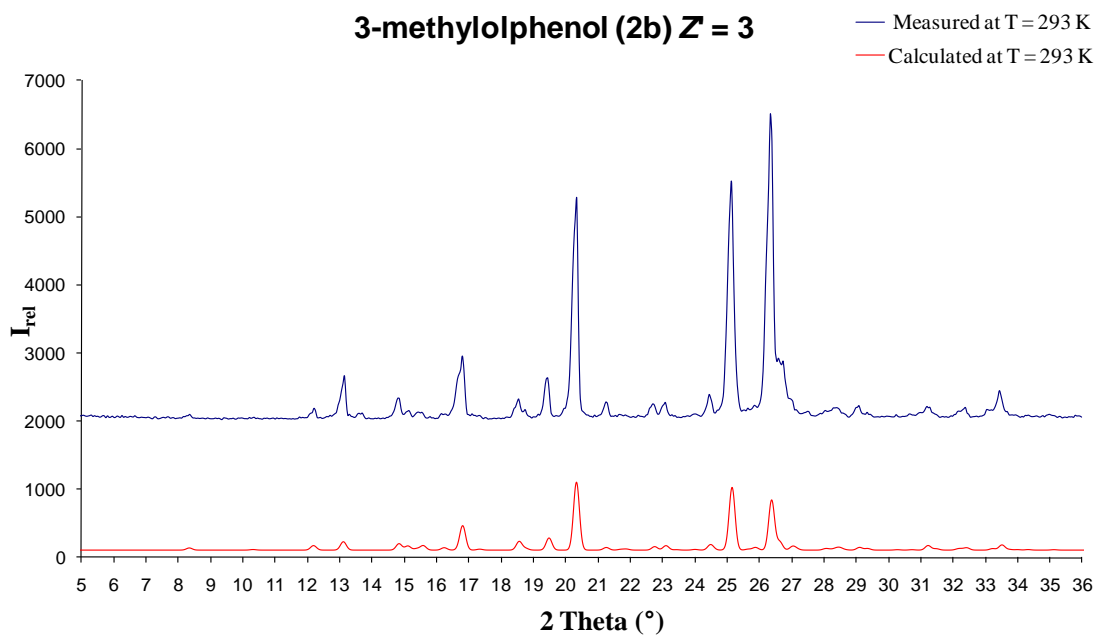
4-methylolphenol (3) from commercial product
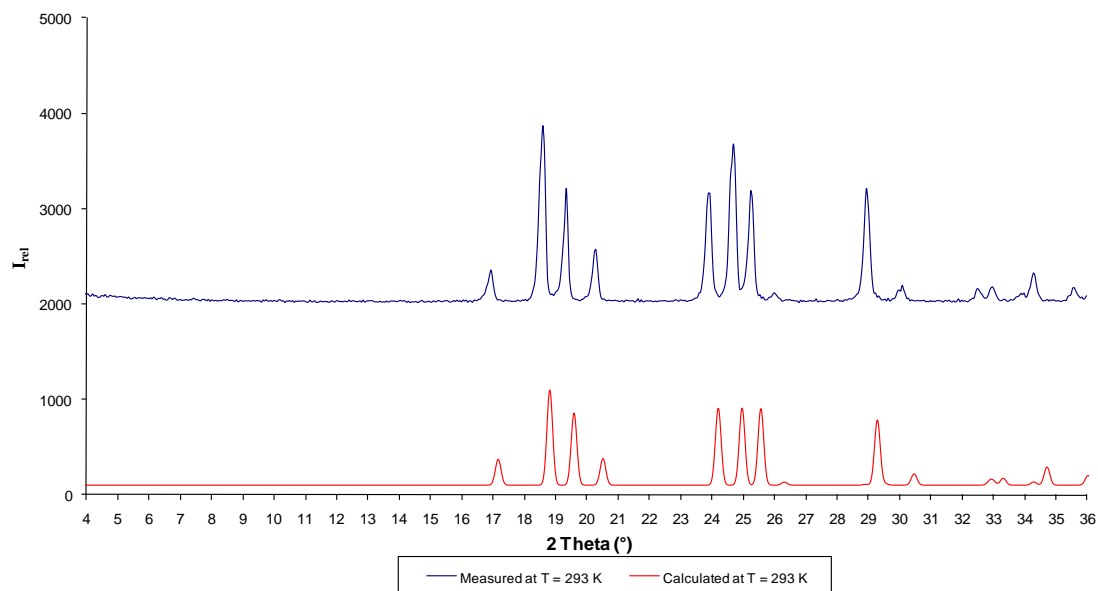
Figure S18: Comparison of powder pattern obtained from commercial product and that calculated from the single crystal structure.

4-methylolphenol (3) from methanol
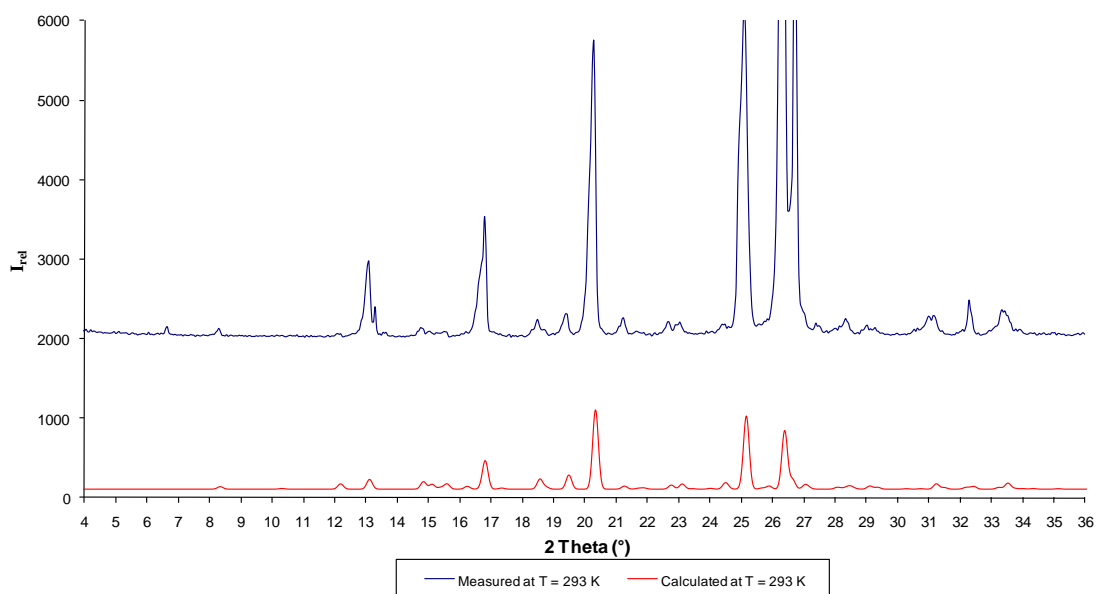

Figure S19: Comparison of powder pattern of crystals grown from methanol and that calculated from the single crystal structure for (**3**).

4-methylolphenol (3) from isopropanol

Figure S20: Comparison of powder pattern of crystals grown from isopropanol and that calculated from the single crystal structure for (**3**).
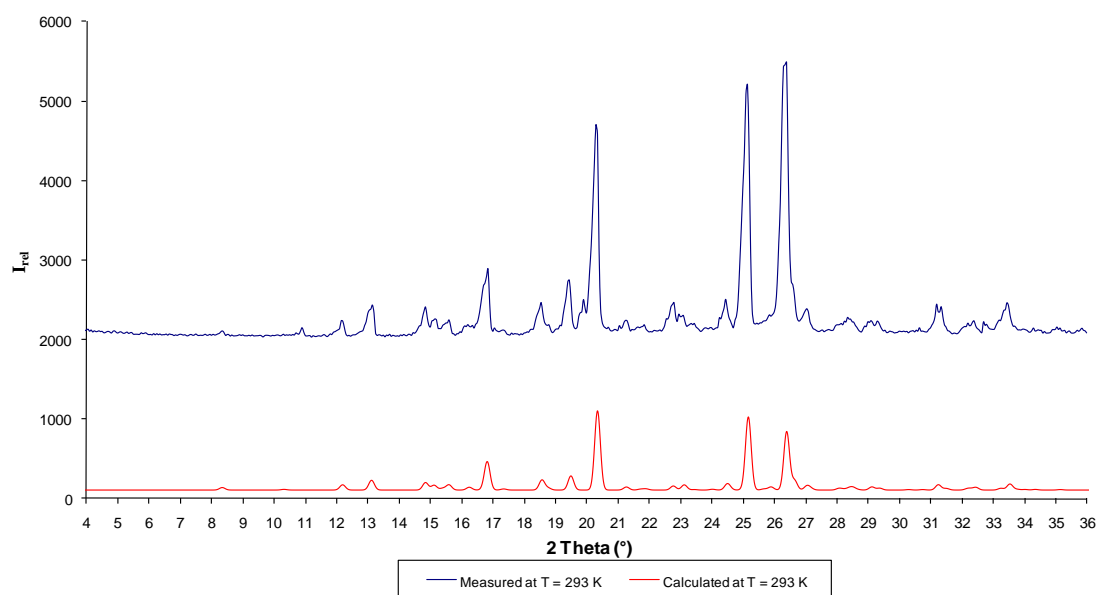
4-methylolphenol (3) from acetonitrile

Figure S21: Comparison of powder pattern of crystals grown from acetonitrile and that calculated from the single crystal structure for (**3**).
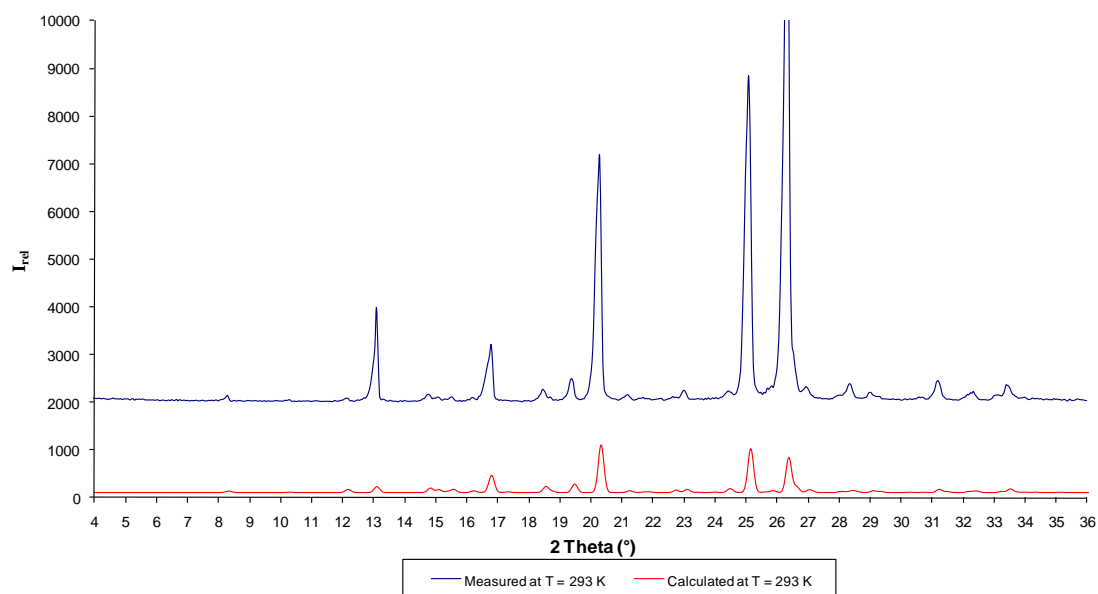
4-methylolphenol (3) from tetahydrofuran
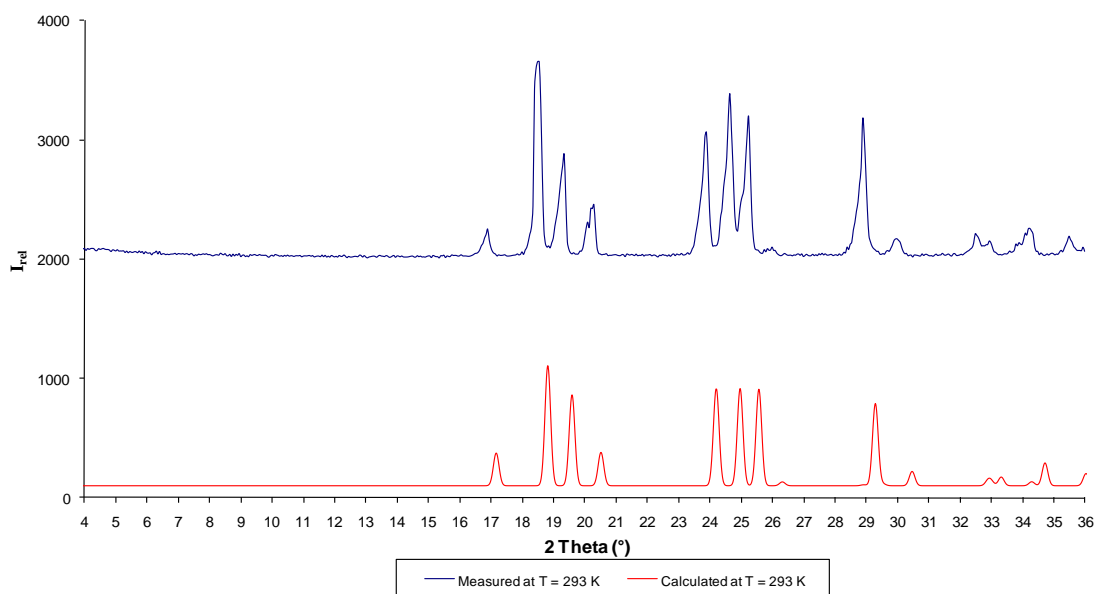
Figure S22: Comparison of powder pattern of crystals grown from tetrahydrofuran and that calculated from the single crystal structure for (**3**).
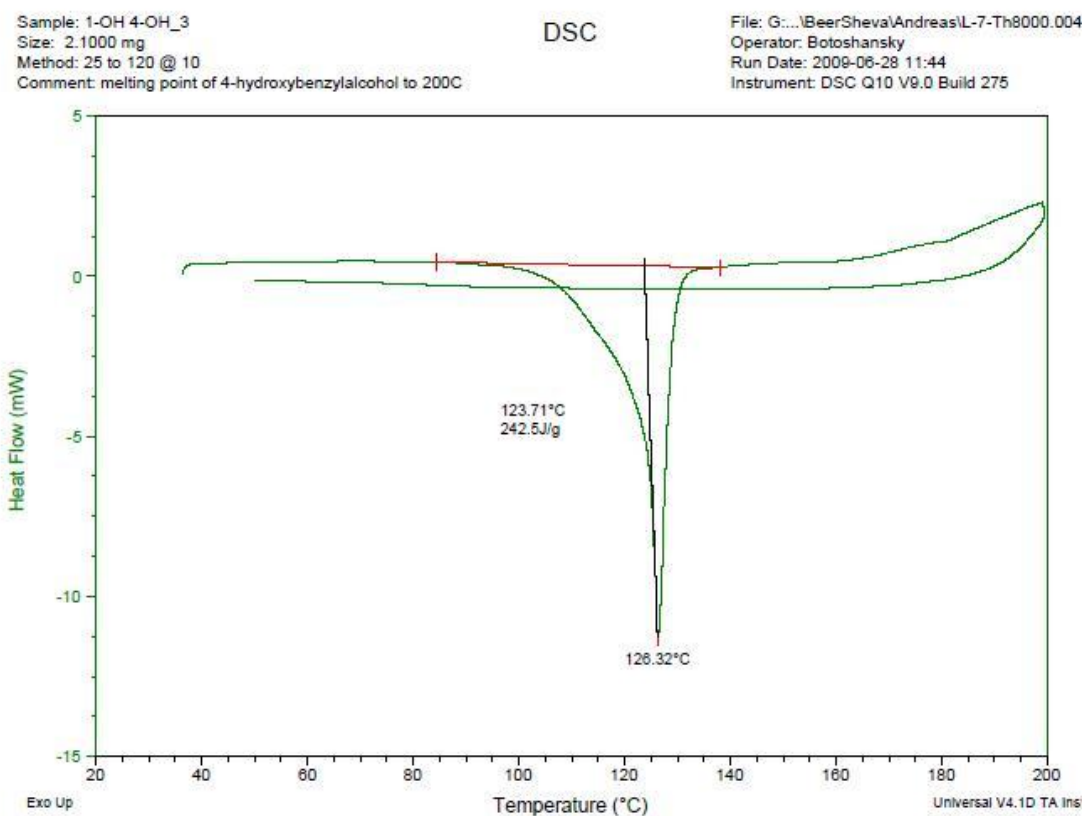
4-methylolphenol (3) from ethyl acetate
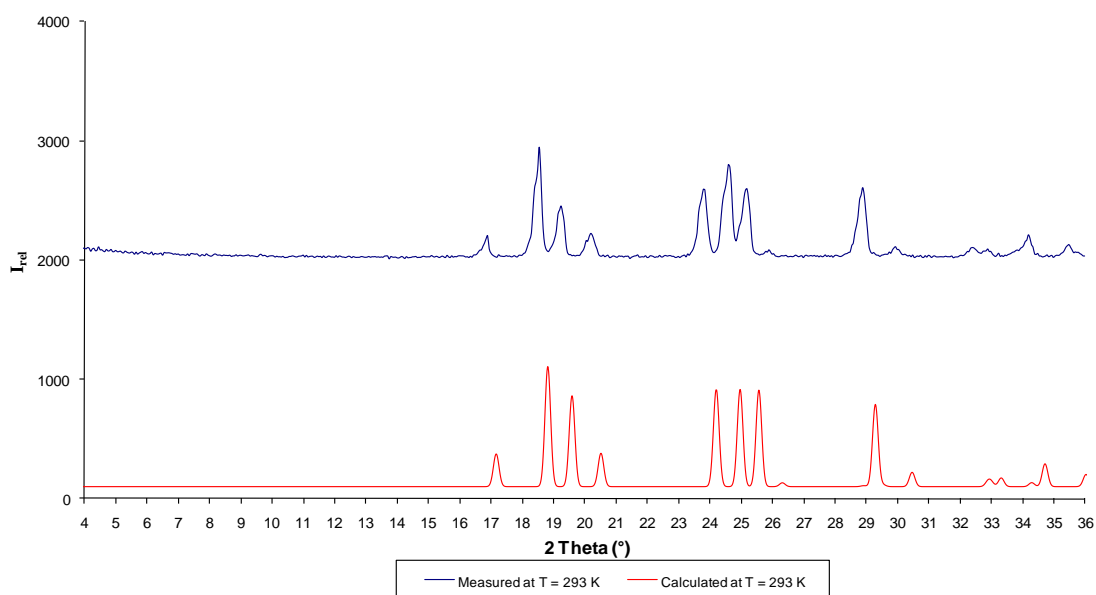
Figure S23: Comparison of powder pattern of crystals grown from ethyl acetate and that calculated from the single crystal structure for (**3**).

4-methylolphenol (3) from acetone
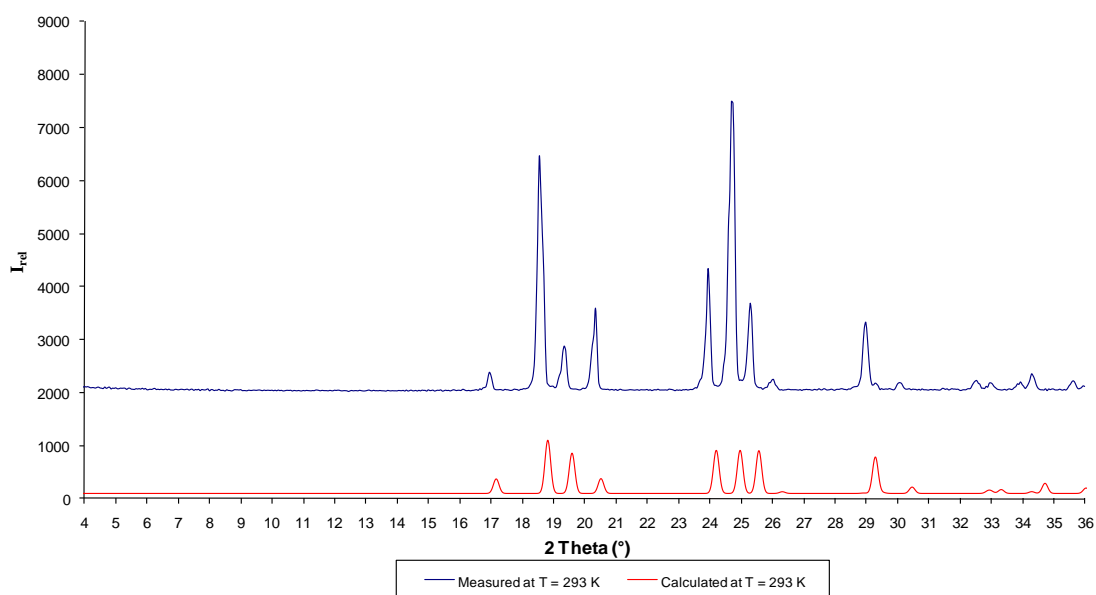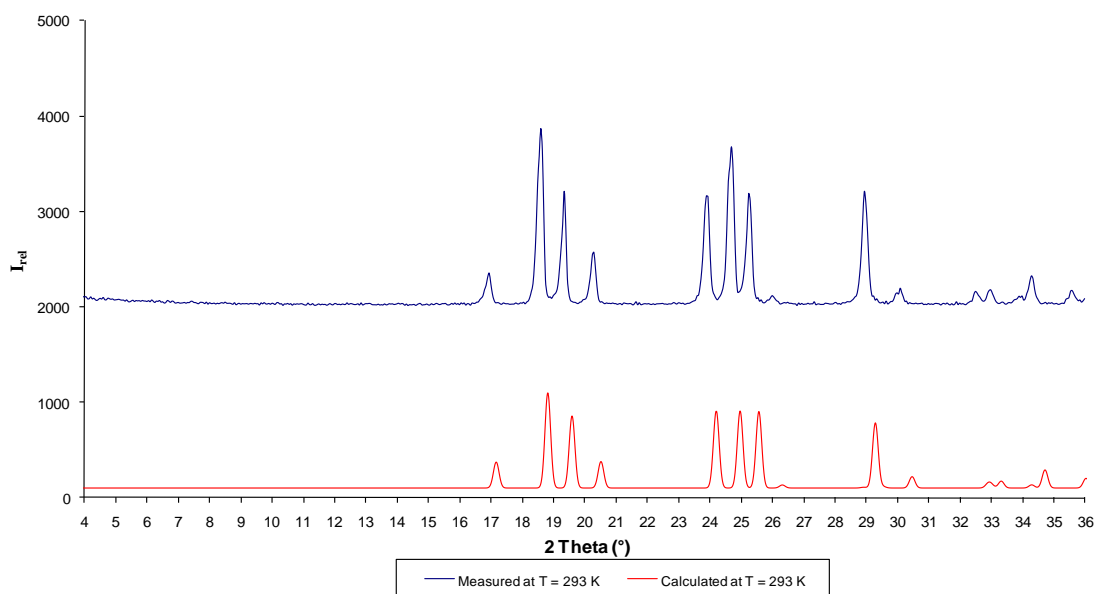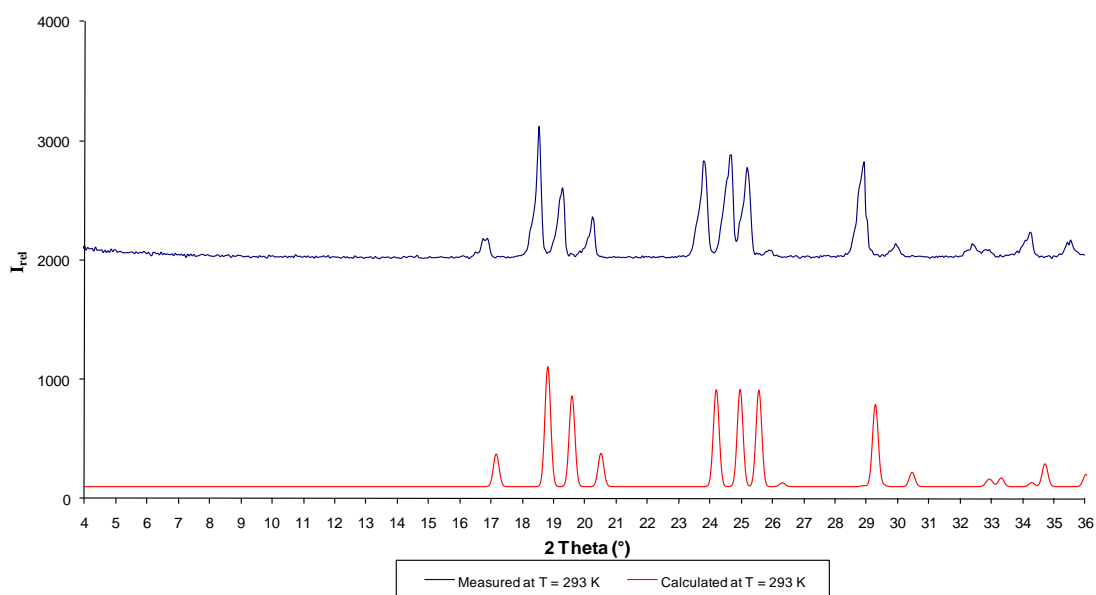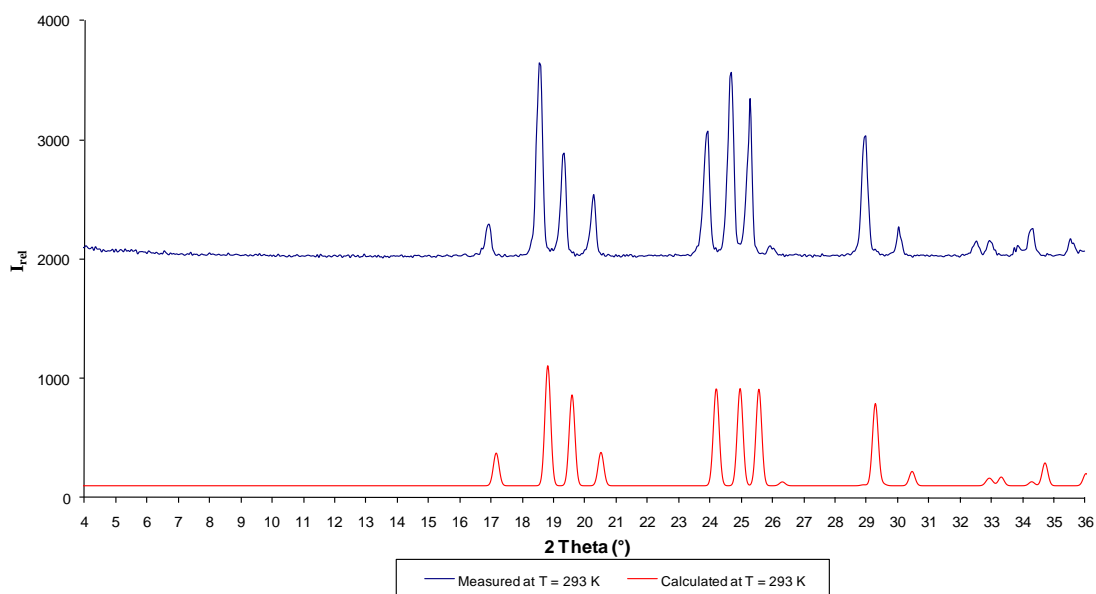

Figure S24: Comparison of powder pattern of crystals grown from acetone and that calculated from the single crystal structure for (**3**).

13

4) Computational results
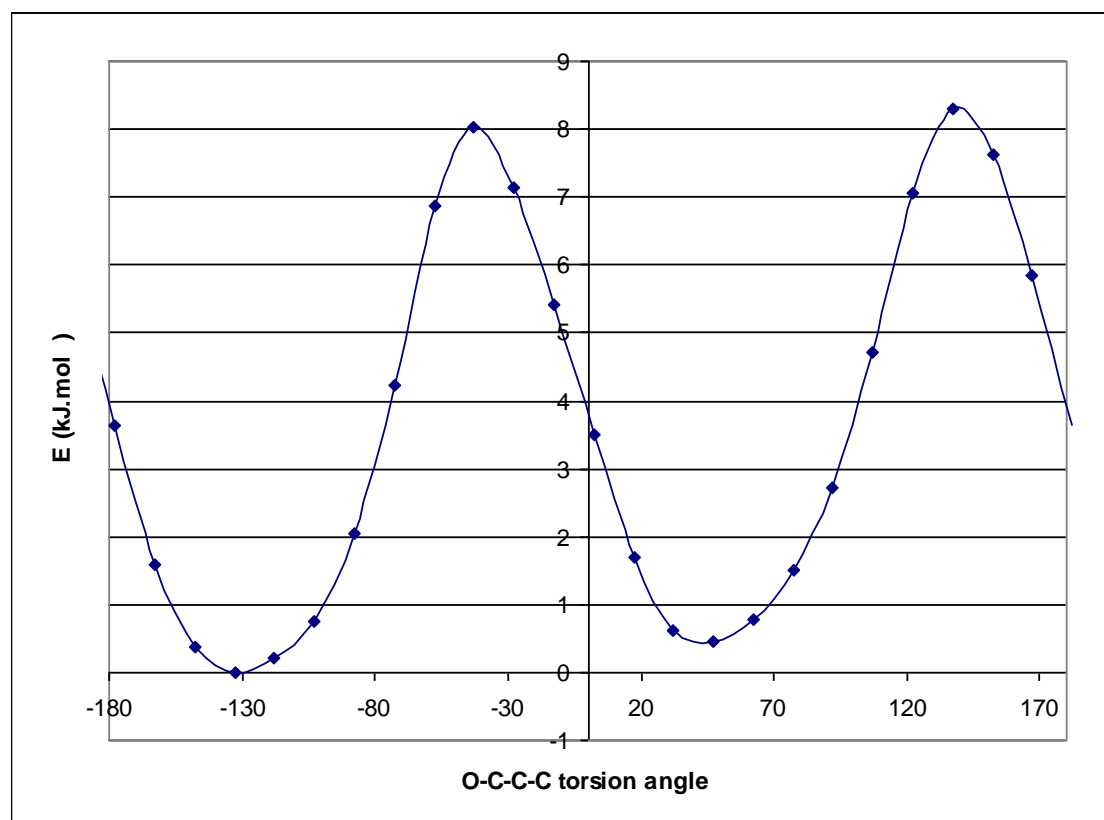
Figure S25: Potential energy scan for rotation around the O-C-C-C torsion angle in **2**, showing the low barrier to rotation (< 9 kJ.mol^{-1})

Table S1 Intermolecular interactions involved in **1 – 3** in kJ.mol^{-1} calculated at the M06-2X/6-31+G(d) level of theory, with H-atom positions optimized at the B3LYP/6-31+G(d) level. Molecules involved in each interaction are placed in the same relative positions as found in the crystal structure. Molecules are numbered according to Figure S26. The total stabilization experienced (in kJ mol^{-1}) by each crystallographically independent molecule is calculated from the individual interactions.

	Interaction*	E (kJ.mol^{-1})	Total stabilization
	1	-34.7	-159.1**
	2	-45.4	
	3	-4.5	
	4	-4.5	
	5	-13.7	
	6	-12.1	
1	7	-3.5	
	8	-3.5	
	9	-0.3	
	10	-4.2	
	11	-12.1	
	12	-13.7	

	13		-1.5	
	14		-2.7	
	15		-2.7	
	16		-34.7	
	Molecule A with			-195.4[**]
	B	(B)	-19.6	
	2	(B)	-30.0	
	4	(A)	-28.1	
	5	A	-28.1	
	6	(B)	-20.4	
	7	(A)	-5.1	
	8	(A)	-20.4	
	9	(A)	-3.4	
	11	(B)	-3.3	
	12	(A)	-5.1	
	13	(B)	-19.6	
	14	(A)	-5.1	
	15	(A)	-2.4	
	16	(B)	-4.3	
2a	18	(B)	-0.5	
	Molecule B with			-175.3[**]
	A	(A)	-19.6	
	1	(A)	-30.0	
	2	(B)	-2.0	
	3	(B)	-27.7	
	4	(A)	-20.4	
	6	(B)	-27.7	
	9	(A)	-3.3	
	16	(B)	-4.0	
	18	(B)	-4.6	
	20	(B)	-4.6	
	21	(A)	-4.3	
	22	(B)	-21.1	
	23	(B)	-4.0	
	24	(B)	-2.0	
	Molecule A with			-146.2[**]
	B	(B)	-19.8	
	3	(C)	-31.3	
	4	(A)	-25.4	
	5	(B)	-20.0	
	6	(C)	-2.4	
	7	(A)	-25.4	
2b	14	(C)	-3.9	
	15	(B)	-3.5	
	16	(B)	-3.2	
	17	(C)	-20.2	
	18	(C)	-2.1	
	19	(B)	-2.9	
	20	(B)	-6.5	
	23	(A)	-0.7	

15

25	(C)	-4.3	
Molecule B with			-199.1**
A	(A)	-19.8	
C	(C)	-19.1	
3	(C)	-1.7	
5	(B)	-27.8	
6	(C)	-19.9	
7	(A)	-20.0	
10	(B)	-27.8	
13	(A)	-2.9	
23	(A)	-6.5	
31	(A)	-3.2	
25	(C)	-4.0	
27	(B)	-5.5	
29	(A)	-20.5	
30	(B)	-20.4	
Molecule C with			-175.1**
B	(B)	-19.1	
6	(C)	-29.2	
8	(C)	-29.2	
7	(A)	-2.4	
10	(B)	-19.9	
13	(C)	-31.3	
31	(A)	-3.9	
33	(C)	-1.7	
34	(A)	-20.2	
35	(C)	-2.4	
36	(B)	-4.0	
37	(A)	-4.3	
38	(C)	-5.4	
39	(C)	-2.1	
1		-15.3	-187.2**
2		-29.4	
3		-6.8	
4		-17.4	
5		-0.3	
6		-6.9	
7		-11.7	
8		-29.4	
9		-6.8	
10		-0.3	
11		-5.8	
12		-5.8	
13		-17.4	
14		-11.7	
15		-6.9	
16		-15.3	

(Row label "3" appears to the left of the numbered block 1–16.)

* Letter in parenthesis indicates conformation of second molecule involved in the interaction.
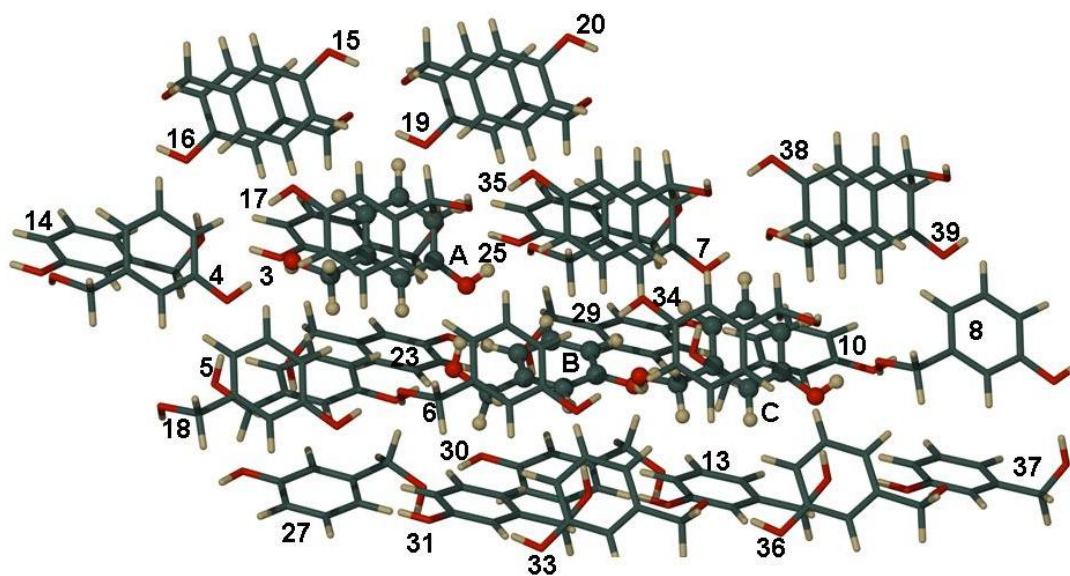
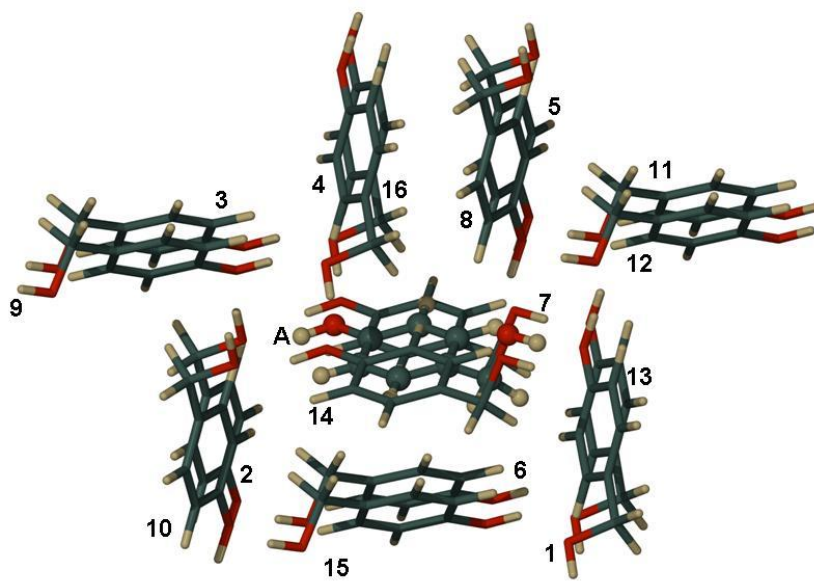** Sum of all interactions with surrounding molecules.
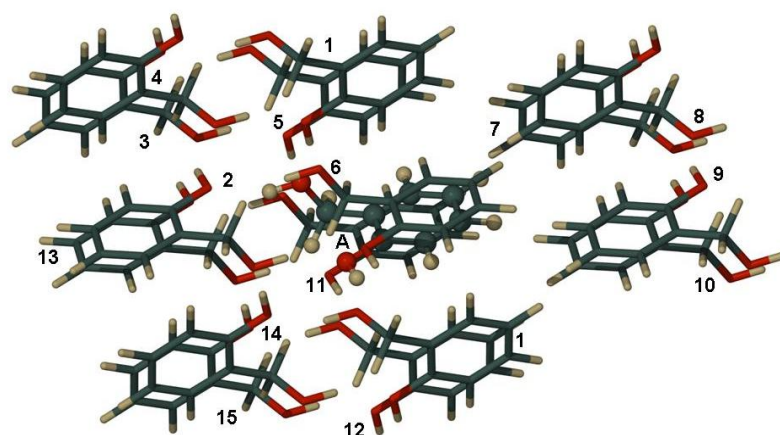
(1)
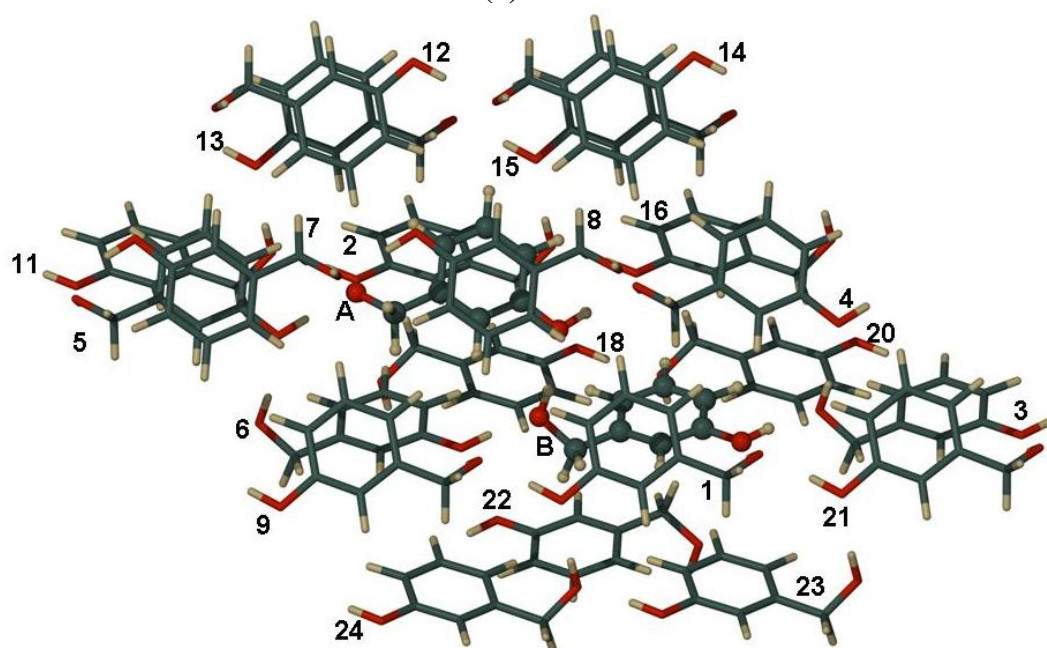
(2a)

(2b)

(3)

Figure S26: Spheres of inclusion around crystallographically independent molecules (A-C, indicated by ball and stick models) for **1 – 3** used to determine all intermolecular interactions referred to in Table S1.